

Possibility of various magnetic configurations in the Cr (Fe) monolayer deposited on vicinal surfaces of Fe (Cr)

A. Vega,* C. Demangeat, and H. Dreyssé

*Institut de Physique et Chimie des Matériaux (IPCMS-GEMME),
UMR 46 du CNRS-Université Louis Pasteur, 23 rue du Loess, 67037 Strasbourg Cedex, France*

A. Chouairi

*Laboratoire de Physique des Solides, Université de Nancy I,
BP 239, Vandoeuvre-les-Nancy, France*

(Received 11 October 1994)

The local magnetic moments and magnetic order are calculated for a Fe (Cr) monolayer adsorbed on semi-infinite Cr (Fe) substrates with high-index surfaces. These stepped interfaces are present in the wedge-shaped configurations recently analyzed by different experimental groups in order to investigate the interlayer magnetic coupling in Fe/Cr/Fe systems. The spin-polarized electronic distribution is obtained by solving self-consistently a *d*-band model Hamiltonian in the mean-field approximation within the framework of the tight-binding real-space method. Several magnetic configurations have been found for all the systems investigated. In the most stable configuration of the Cr monolayer on Fe vicinal surfaces, the local moments of most of the Cr atoms are antiferromagnetically coupled with the Fe moments, an exception being the Cr atoms at the edge of the step. Cr atoms at nearest-neighbor positions (located at the kink and edge of the steps) are always antiferromagnetically coupled. For the Fe monolayer on Cr vicinal surfaces, the average magnetization at the surface results is zero for the two most stable solutions. However, other metastable solutions with net average magnetization on the Fe overlayer are found. The Fe atoms at the edge and kink of the steps (first neighbors) are, in all cases, ferromagnetically coupled. These results are in qualitative agreement with recent experimental observations.

I. INTRODUCTION

Considerable attention has been devoted in the last years to find a physically transparent explanation of the exchange coupling between adjacent Fe layers across a Cr spacer and of the local magnetic polarization at the Fe/Cr interface. The possibility of tailoring new materials with properties of technological interest like controlled magnetization and magnetic ordering, as well as giant magnetoresistance, has opened new prospects in surface physics. In 1979, Allan¹ pointed out an enhanced polarization at the (001) surface of Cr. This result was confirmed later on from both experimental² and theoretical^{3,4} sides. Enhancement at the surface of Fe(001) and Fe(101) was also obtained by Freeman and co-workers.^{5,6} More recently antiferromagnetic exchange coupling of adjacent Fe layers through Cr layers was shown by Grünberg *et al.*⁷ through light-scattering and by Baibich *et al.*⁸ through magnetoresistance experiments. Besides oscillations from ferromagnetic (F) to antiferromagnetic (AF) exchange couplings with a long period, Unguris, Celotta, and Pierce⁹ and Purcell *et al.*¹⁰ have found oscillations with a period of two Cr monolayers when the crystallographic quality of the interfaces is good. The coupling was measured on a sample consisting of an Fe(001) single-crystal whisker substrate and a Cr wedge deposited by molecular beam epitaxy and covered by the Fe overlayer. As discussed in those papers^{9,10} (See, for example, Fig. 1 of Ref. 9), the polarization of

the Fe overlayer changes from step to step (with a period of two monolayers).

The magnetization of Cr overlayers deposited on Fe (and Fe overlayers on Cr) has been also widely investigated but it is far from being completely understood. The tight-binding calculations of Victora and Falicov³ and the full-potential linearized-augmented-plane-wave (FLAPW) results of Fu *et al.*⁴ predicted strongly enhanced magnetic moments for one monolayer of Cr deposited on the ideal Fe(001) surface, as well as an antiparallel orientation of the Cr and Fe moments. The predicted giant moments were recently obtained by Turtur and Bayreuther¹¹ from *in situ magnetometer measurements* during the growth of ultrathin Cr films on Fe(001). The Cr moments in the first atomic layer are aligned antiparallel to the Fe moments, but complex magnetic behaviors at the interface are suggested by these experimental results. A ferromagnetically ordered monolayer of Cr on Fe(001) oriented antiparallel to the Fe moments has been also obtained through spin-polarized core-level photoemission¹² and soft x-ray magnetic circular dichroism.¹³ In contrast to the above experimental results, sputtered Cr films on Fe were investigated via the polarization of secondary electrons generated by an unpolarized electron beam of 1 keV energy, and an upper limit of $0.01\mu_B$ was set on the Cr moments.¹⁴ The magnetism at the surface of a Cr film grown epitaxially on a Fe(001) whisker has been observed as a function of the Cr thicknesses by scanning electron microscopy with

polarization analysis¹⁵ (SEMPA) and by spin-polarized electron-energy-loss spectroscopy¹⁶ (SPEELS). The surface magnetic moments change their direction with each additional Cr layer. With respect to Fe deposited on Cr, the magnetization behavior of thin epitaxial Fe films on Cr(100) has been recently investigated through the magneto-optical Kerr effect by Berger and Hopster.¹⁷ The main result is a sharp transition of the coercive field, independent of film thickness. The origin of this transition is attributed to a spin-flip transition in Cr. This experimental study presents an example of how the Cr substrate can influence the properties of an adjacent Fe layer through the interface exchange coupling. These authors suggest a possible explanation for this effect given by a simple model taking into account a nonideal (100)-interface structure. Another question of interest is the presence of "apparent" dead layers when a few Fe monolayers are grown on Cr(001).^{18,19}

Up to now, the theoretical predictions are based on ideal surfaces and interfaces, whereas structural defects (steps, vacancies, reconstruction) occur in the growth process. Indeed, steps of monoatomic height at the (001) surface of Cr have been monitored by a scanning tunnel microscope²⁰ (STM) and can describe the "real" Cr(001) surface. Since Fe and Cr are known to be very sensitive to changes in their local geometrical and chemical environment, an interesting variety of magnetic behaviors is expected as soon as these defects appear at the surfaces and interfaces. Motivated by the above facts, the aim of the present work is to shed light on this complex subject by analyzing the spin polarization (local magnetization and magnetic order) of an Fe (Cr) monolayer adsorbed on semi-infinite Cr (Fe) substrates containing step like defects of different sizes. The results presented here give compelling evidence that the presence of such types of defects at the surface of the substrates is at the origin of some of the curious magnetic behaviors experimentally observed. In this respect, some of the discrepancies in the experimental findings can be traced back to these irregularities at the surfaces during the growth process.

The spin-polarized electronic charge distribution is calculated by using a self-consistent tight-binding model in combination with the recursion method in the real space.²¹ These types of calculations have given, in the case of periodic systems like Fe/Cr superlattices or Fe/Cr/Fe sandwiches,^{22,23} satisfactory agreement with methods using the local density approximation²⁴ (LDA). Moreover, the more sophisticated *ab initio* calculations based on the LDA are rarely applied to vicinal surfaces or to extended defects, with the exception of the calculation of Hampel, Vvedensky, and Crampin²⁵ about magnetic structure near (310) tilt boundaries in Fe, using the layer-Korringa-Kohn-Rostocker (LKRR) method. As discussed recently by Lee and Callaway,²⁶ Cr clusters can present more than one magnetic state. Since the solution of our model is not unique, we have looked for different magnetic arrangements at each of the systems, and we have calculated the total energy difference between them.

The rest of the paper is organized as follows. In Sec. II, we present our theoretical model. Section III is devoted

to the study of the monolayer of Cr deposited on vicinal Fe(1,0,2*n* - 1) surfaces. In Sec. IV we discuss the results for a monolayer of Fe on vicinal Cr(1,0,2*n* - 1) surfaces. Our results are analyzed in connection with recent experiments by Unguris, Celotta, and Pierce,⁹ Purcell *et al.*,¹⁰ and Turtur and Bayreuther.^{11,19} Section V summarizes our conclusions.

II. THEORETICAL MODEL

The magnetic moment distribution at $T = 0$ K of these semi-infinite systems, composed by a large number of inequivalent sites of Fe and Cr, is determined by solving self-consistently a *d*-band model Hamiltonian in a mean-field approximation. Our tight-binding Hamiltonian is written in the usual notation as

$$H = \sum_{i\alpha\sigma} \varepsilon_{i\sigma} \hat{n}_{i\alpha\sigma} + \sum_{\substack{\alpha\beta\sigma \\ i \neq j}} t_{ij}^{\alpha\beta} \hat{c}_{i\alpha\sigma}^\dagger \hat{c}_{j\beta\sigma}. \quad (1)$$

Here, $\hat{c}_{i\alpha\sigma}^\dagger$, $\hat{c}_{i\alpha\sigma}$, and $\hat{n}_{i\alpha\sigma}$ refer to the creation, annihilation, and number operators of an electron with spin σ at the orbital α of atomic site i ($\alpha \equiv d_{xy}, d_{yz}, d_{zx}, d_{x^2-y^2}, d_{3z^2-r^2}$). We consider spin-independent hopping integrals $t_{ij}^{\alpha\beta}$ up to next-nearest neighbors. These elements $t_{ij}^{\alpha\beta}$ are obtained from the Slater-Koster two-center integrals $dd(\sigma, \pi, \delta)$, which we assume to vary as the inverse of the fifth power of the interatomic distance R_{ij} between i th and j th neighbor atoms. In this way,

$$dd(\sigma, \pi, \delta)_{ij} = (6, -4, 1) dd(\delta)_{\text{bulk}} (R_{\text{bulk}}/R_{ij})^5, \quad (2)$$

where the two-center hoppings corresponding to the bulk interatomic distance (R_{bulk}) are chosen in order to recover the *d*-band width of Varma and Wilson.²⁷ Since the overlayer is assumed to adopt the substrate's interatomic distance, we scale the hopping integrals between atoms belonging to the overlayer to the lattice parameter of the substrate accordingly with Eq. (2). At the Fe/Cr interface, the heteronuclear hoppings $dd(\sigma, \pi, \delta)_{\text{Fe-Cr}}$ are approximated by the geometrical average of the corresponding homonuclear hoppings:

$$dd(\sigma, \pi, \delta)_{\text{Fe-Cr}} = \sqrt{dd(\sigma, \pi, \delta)_{\text{Fe-Fe}} \times dd(\sigma, \pi, \delta)_{\text{Cr-Cr}}}. \quad (3)$$

The spin-dependent diagonal terms of the Hamiltonian are given by

$$\varepsilon_{i\sigma} = \varepsilon_i^0 + \Omega_i - z_\sigma \frac{J_i}{2} \mu_i, \quad (4)$$

where i refers to the atomic sites in the system and z_σ to the spin ($z_\uparrow = +1$; $z_\downarrow = -1$). ε_i^0 is the *d*-energy level in the paramagnetic solution of the bulk corresponding to the element (Cr or Fe) at site i . The site-dependent term Ω_i accounts for the shift of the energy level due to direct Coulomb interactions, to nonorthogonality effects, and to the variation of the crystal-field potential of the neighboring atoms.²⁸ In the present work, as in our recently reported study of V overlayers on semi-

infinite Fe,²⁹ we consider local charge neutrality by adjusting self-consistently these potentials Ω_i with the requirement that the electronic occupation of each atom be the same as in the corresponding bulk. The local neutrality condition has proved to be a good approximation for these materials.^{3,30} A recent study by Vega *et al.*³¹ for Fe nanoparticles embedded in Cr gives a very small charge transfer (of the order of 0.05 d electrons) between the inequivalent sites. Finally, the third term in Eq. (4) stands for the shifts due to intra-atomic Coulomb interactions. The exchange parameters J_i (i =Fe,Cr) are chosen so as to recover the Fe bulk magnetization ($2.21\mu_B$) and the antiferromagnetic state of bulk Cr with the corresponding local magnetization ($0.60\mu_B$).

The number of electrons, N_i , and the local magnetic moments, μ_i , at site i , given by

$$N_i = N_{i\uparrow} + N_{i\downarrow} \quad (5)$$

and

$$\mu_i = N_{i\uparrow} - N_{i\downarrow}, \quad (6)$$

are determined self-consistently by requiring

$$N_{i\sigma} = \langle \hat{n}_{i\sigma} \rangle = \int_{-\infty}^{\epsilon_F} \sum_{\alpha} \rho_{i\alpha\sigma}(\epsilon) d\epsilon. \quad (7)$$

The local density of states (LDOS) at site i , for the orbital α and spin σ , $\rho_{i\alpha\sigma}(\epsilon)$, is calculated by using the recursion method in real space.²¹ The number of levels of the continued-fraction expansion of the Green functions is 12 so that the results become independent of it.

Before presenting the calculations we would like to be precise as to how sensitive is our model to a variation in the parameters. With respect to the hopping integrals, we have considered a variation of about 10% in the relative hybridization between the Cr and Fe bands. The quantities of interest, i.e., local magnetic moments and magnetic order, do not change qualitatively. The trends are, thus, the same independently of the choice of the hoppings within this range, although a small difference [of the order of (0.1–0.2) μ_B] was obtained in the values of the local magnetic moments. For the Cr/Fe(1,0,2 n –1) systems, we have performed the self-consistent calculation in all the inequivalent atoms of the Cr overlayer and three Fe layers. Below the third layer, the spin-dependent electronic distribution of bcc Fe is assumed. This has proved to be a good approximation, since subsequent tests considering four and five Fe layers as different from the bulk give no variation in the local moments close to the interface. The same holds for the total-energy differences between the different magnetic configurations. For Fe/Cr(1,0,2 n –1), six Cr layers have to be considered as different from the Cr bulk. In this case, the convergence to the bulk distribution is slower than for the Fe substrate due to the larger number of unpolarized d holes of Cr which makes it more sensitive than Fe to changes in the local environment, as discussed in the following sections.

III. MAGNETISM OF A Cr MONOLAYER ON VICINAL SURFACES OF Fe

In this section we investigate the magnetic properties of a Cr monolayer on vicinal Fe(1,0,2 n –1) surfaces. For $n = 1$ and $n \rightarrow \infty$, these surfaces correspond to the low-index (101) and (001) crystallographic faces, respectively. The rest of surfaces investigated ($n = 2, 3, 4, 5, 6$) correspond to intermediate orientations and can be seen as (001) surfaces with terraces of monoatomic height and a length in the x direction of n atomic rows parallel to the y direction. For the (101) orientation, the average magnetization per atom at the Cr overlayer is nearly zero, whereas for the (001) crystallographic face, the magnetic moment of Cr is $-2.51\mu_B$, and the moment of Fe at the subsurface plane is equal to $1.78\mu_B$.

For the stepped surfaces, a large variety of magnetic arrangements is possible. This arises from the fact that in the presence of these structural defects, it is not possible to preserve the ferromagnetic order between all Fe-Fe nearest neighbors and, at the same time, a perfect antiferromagnetic coupling between all Fe-Cr and Cr-Cr nearest neighbors. The reason is that the atoms at the interface do not belong to a single magnetic sublattice of an antiferromagnetic bcc system. Therefore, frustrated nearest-neighbor bonds are present, and different solutions are obtained when these “magnetic defects” are located at different areas of the system.

As in the case of V/Fe(1,0,2 n –1),^{29,32} a “single-cell” periodic configuration (one step as the periodic cell) is obtained due to the strong ferromagnetism of the Fe substrate. On the contrary, at the surface of pure V (Ref. 33) or at the surface of pure Cr (Ref. 34), the “double-cell” configuration (two steps as the periodic cell) is more favorable than the single cell due to the antiferromagnetism of Cr and the tendency towards the AF order observed in V.

In Fig. 1, the magnetic moment distribution is shown for the most stable solution of Cr/Fe(1,0,2 n –1) for $n = 2, 3, 4, 5, 6$. In this magnetic configuration, only the row [parallel to the (010) direction] of Cr atoms at the edge of the step and one row of Fe atoms at the interface are frustrated (i.e., ferromagnetically coupled) per step. The rest of the atoms preserves the normal coupling. Thus, most of the Cr atoms are antiferromagnetically coupled with Fe. The magnetic defect is very localized in this case and does not propagate into the Fe substrate. It is interesting to note that the Cr atoms located at the edge of the step (the less coordinated ones) do not display the largest local magnetic moments except for $n = 2$. This behavior was also obtained in the case of V/Fe(1,0,2 n –1),^{29,32} in contrast to the pure Cr(1,0,2 n –1) and pure Fe(1,0,2 n –1) systems. The importance of a good description of the local symmetry (chemical and geometrical environment) is, thus, evident. The simple rule of the coordination number (the less coordinated atom displays the largest magnetization) does not always apply, and an accurate determination of the local densities of states is necessary. Due to the strong sensitivity of Cr to the changes in the environment, the convergence of the moment of the central atoms of the

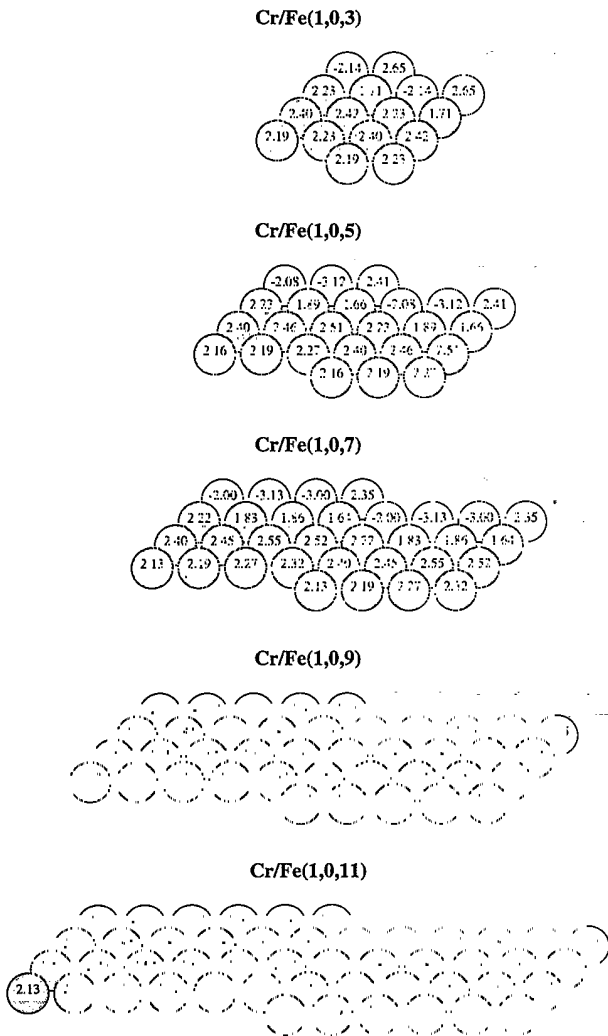


FIG. 1. Local magnetic moments, in units of μ_B , for the most stable solution obtained for $\text{Cr/Fe}(1,0,2n-1)$ when $n = 2, 3, 4, 5, 6$. The white circles represent the Cr atoms, whereas the dashed circles represent the Fe atoms. Notice that only a portion of the semi-infinite system in its bcc structure is illustrated as a projection on the (010) plane.

steps towards that of the ideal $\text{Cr/Fe}(001)$ is very slow. For instance, for $n = 6$ we obtain $-2.72\mu_B$ at the center of the step whereas at the (001) it reduces up to $-2.51\mu_B$. A quantity of interest from the experimental point of view is the average magnetization. In Fig. 2, the average magnetization per atom is shown as a function of the step-length n for this magnetic configuration. Many experimental techniques are able to determine the spin polarization within the first two to three layers below the surface. For this reason we give, together with the average magnetization per surface atom, the values calculated by considering in the average the first and the second Fe layers below the surface. Although for $n = 2$ the average magnetization at the surface has the same sign as for the Fe substrate, a transition to an antiparallel average spin polarization is obtained for $n = 3$. We can appreciate how slow the convergence is to the values of the ideal $\text{Cr/Fe}(001)$ system. These results in-

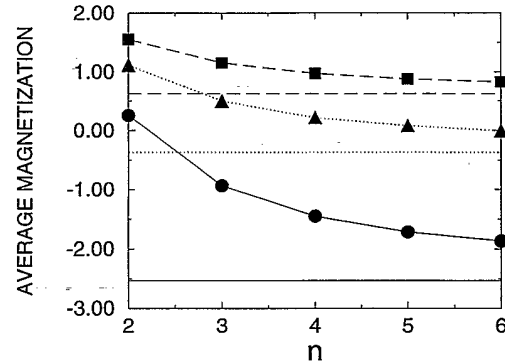


FIG. 2. Average magnetization per atom in the most stable solution of $\text{Cr/Fe}(1,0,2n-1)$ as a function of the step length. Circles: only the Cr surface atoms are taken into account. Triangles: the Cr surface atoms and the first Fe subsurface layer are considered in the average. Squares: the Cr surface atoms and the two first Fe layers are considered in the average. The horizontal lines represent the corresponding values for the ideal $\text{Cr/Fe}(001)$.

dicates that the presence of this type of structural defects leads to a reduction of the spin polarization of the system and that the magnetic interactions between the steps remain even for very long step lengths. For $n \geq 5$, the results obtained here are in good agreement with recent *energy-resolved spin-polarized secondary electron emission* experiments,³⁵ which give a moment of $1.8\mu_B$ for the Cr overlayer, antiferromagnetically coupled with Fe.

Other magnetic configurations are also obtained as a solution of our model. In Fig. 3, for instance, these are shown for $\text{Cr/Fe}(1,0,7)$ [solution (a) is the one discussed in Fig. 1]. In all cases, the Cr atoms located at the kink and at the edge of the step (nearest neighbors) are antiferromagnetically coupled. When we start as input with a double-cell arrangement in which the nearest-neighbor Cr-Cr bonds are frustrated, a spin flip occurs during the self-consistent procedure arriving to one of the solutions of Fig. 3. This happens for all the step lengths analyzed. The solutions obtained differ in the number of Fe-Cr frustrated bonds and in the position of the magnetic defect which is very localized and does not affect drastically the Fe substrate. In all the solutions, the magnetic defect presents the symmetry in the y direction imposed by the structural defect. In solution (b), three Fe-Cr bonds are frustrated per step, one at the kink and the two others at the center of the step (in rows parallel to the y direction). In solutions (c) and (d), two and four Fe-Cr bonds are frustrated, respectively.

Although the magnetic order in the Fe substrate remains ferromagnetic for all the solutions, at the Cr overlayer two different orderings are found. In solutions (a) and (c), all Cr atoms display a local magnetic moment pointing in the same direction (and opposite to the Fe moment), except the Cr atoms at the edge and at the kink, respectively. In contrast, an alternating positive and negative local moments at the Cr overlayer is obtained in configurations (b) and (d). The particular mag-

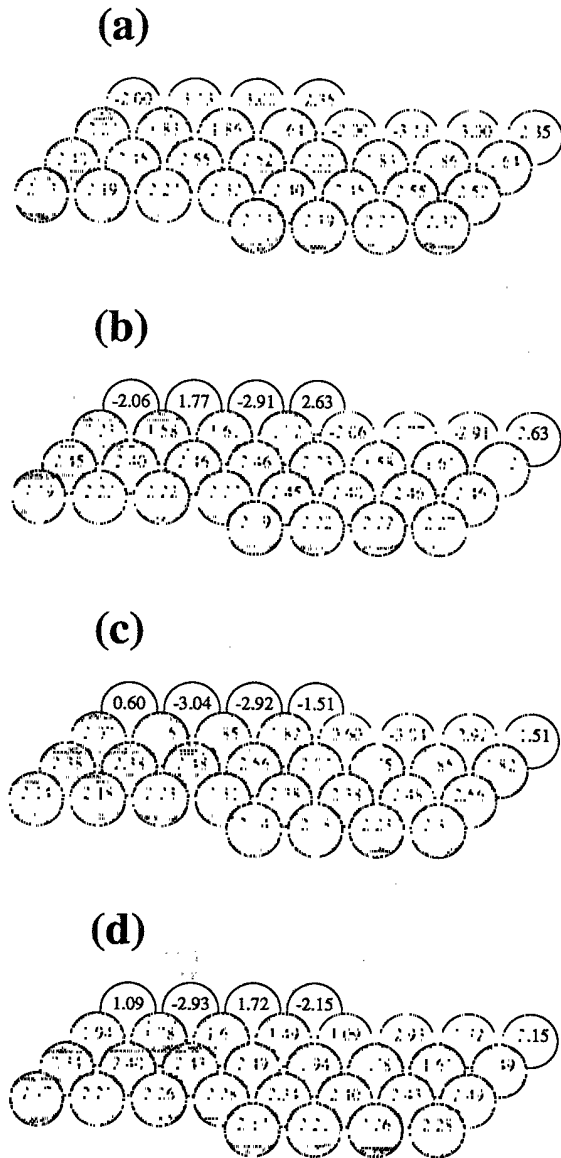


FIG. 3. Various magnetic arrangements found for Cr/Fe(1,0,7). Notice that solution (a) corresponds to that shown in Fig. 1.

netic moment distribution obtained in each solution gives rise to a different average magnetization, as shown in Table I. In Table I we give also the difference in the total energy between the metastable solutions [(b), (c), (d)] and the more stable one [(a)] which is taken as the reference. The average magnetization in the Cr overlayer is much smaller in the antiparallel solutions (b) and (d) than in the parallel (a) and (c), but in all cases opposite to the moment of the Fe substrate. When the first and second Fe layers are included in the average, the antiparallel solutions (b) and (d) display the largest value for the average magnetization. The difference in the total energy between the various solutions is found to be small (see Table I) and very localized in the surrounding

TABLE I. Average magnetization per atom in the four solutions found for Cr/Fe(1,0,7) and shown in Fig. 3. $\bar{\mu}_i$ is the magnetization per atom when $(i - 1)$ Fe layers are averaged with the Cr overlayer. Difference in total energy (ΔE) between the metastable solutions and the stable configuration (a) taken as a reference. The difference in energy is calculated per step.

Configuration	(a)	(b)	(c)	(d)
$\bar{\mu}_1$ (μ_B)	-1.45	-0.14	-1.72	-0.57
$\bar{\mu}_2$ (μ_B)	0.22	0.82	0.08	0.57
$\bar{\mu}_3$ (μ_B)	0.97	1.36	0.87	1.18
ΔE (eV)	0.00	0.09	0.14	0.18

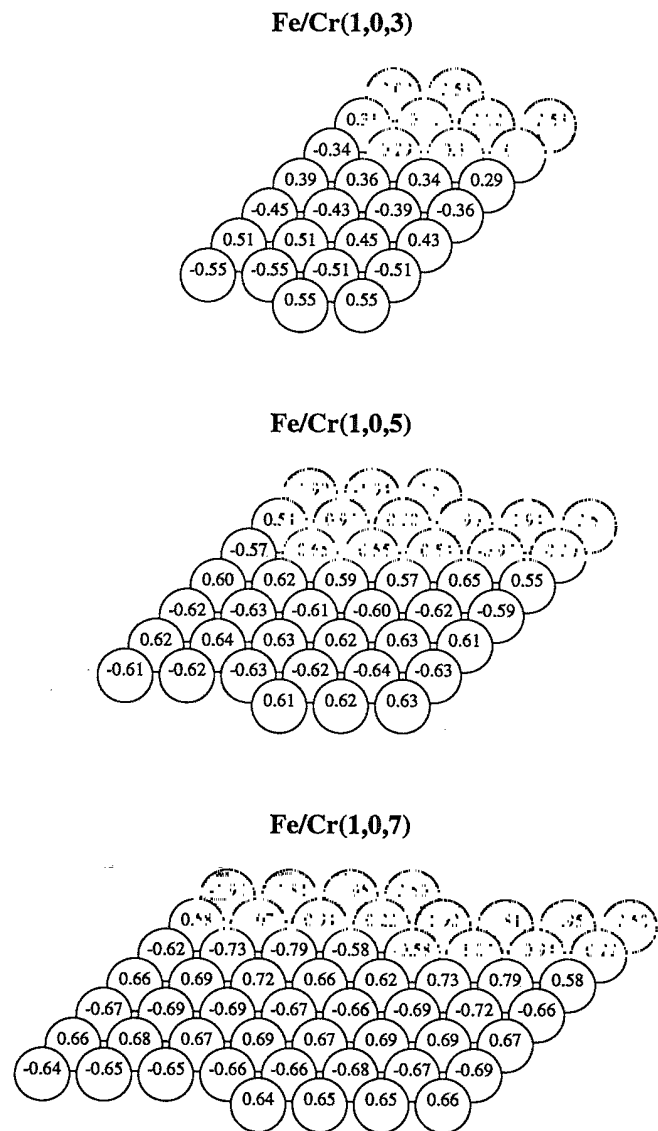


FIG. 4. Local magnetic moments, in units of μ_B , for one of the most stable solutions obtained for Fe/Cr(1,0,2n - 1) when $n = 2, 3, 4$.

of the defect. Taking into account that most of the experiments are performed at room temperature (≈ 0.025 eV) and that our differences in energy are calculated at $T = 0$ K, one can conjecture that some of these magnetic arrangements may coexist in the presence of such structural defects. The large variety of experimental observations (apparently controversial) at these systems, such as the absence of magnetization or the detection of a net spin polarization at the surface, is very indicative in this context. Finally, it is interesting to note that although solution (a) is the most stable for all the step lengths, the relative stability of solutions (b) and (c) changes for larger step lengths, (c) becoming more stable than (b) for $n = 6$. Besides, a parity effect is present in the antiparallel solutions of type (b) and (d) which do not exist for $n = 3$ and $n = 5$ because they give rise to nearest-neighbor Cr-Cr frustrated bonds. In these cases, other solutions in between the parallel and antiparallel configurations of the type shown for Cr/Fe(107) are possible.

IV. MAGNETISM OF AN Fe MONOLAYER ON VICINAL SURFACES OF Cr

For the Fe/Cr(101), the ground state consists of an in-plane antiferromagnetic configuration for both Fe and Cr layers in the (101) crystallographic face. This configuration is indeed "natural" for Cr since it is characteristic of bulk Cr for each (101) crystallographic face. The hybridization between the Fe and Cr d orbitals together with the antiferromagnetic ordering lead to a reduction of the Fe magnetization ($1.34\mu_B$) with respect to the bulk. The magnetization of Cr in the subsurface layer is also smaller ($0.45\mu_B$) than in the Cr bulk. For Fe/Cr(001), the Fe atoms are ferromagnetically coupled within the plane, but antiferromagnetically coupled to the Cr atoms. The polarization at the Fe atoms is also smaller ($1.60\mu_B$) than in the Fe bulk, but the magnetic moment at the Cr subsurface is higher ($2.0\mu_B$) than in the Cr bulk.

Let us now discuss the results obtained for high-index Fe/Cr(1,0,2n-1) systems. In Fig. 4, we show the most stable configurations obtained for $n = 2, 3, 4$. Figure 5 displays the different solutions found for the Fe/Cr(1,0,7) system, taken as an example. A double-cell configuration (two steps as the periodic cell) is always obtained in these systems due to the antiferromagnetic order of the Cr substrate. The solution of Fig. 4, which corresponds to solution (b) of Fig. 5, is degenerated with (a) (see Table II below). The frustration in (b) occurs between the row of Fe atoms located at the edge of the step and one row of Cr atoms at the interface, as was the case in the most stable solution of Cr/Fe(1,0,2n-1). In the different solutions obtained, all the Fe atoms, except the edge atoms, exhibit local magnetic moments smaller than in the bulk. This is due to the presence of the Cr substrate [the smaller exchange splitting of Cr (Ref. 29) and the hybridization between Fe and Cr orbitals tends to decrease their magnetic moment]. The Fe atoms at the edge of the step, which have less Cr neighbors and smaller local coordination number, display a local magnetic moment greater than in the bulk and also greater

than in the ideal Fe/Cr(001) system. The above holds for all the solutions found (see Fig. 5). An important difference with respect to the Cr/Fe(1,0,2n-1) is that the Cr substrate is much more sensitive to the magnetic defect than the Fe substrate. Indeed, we obtain a considerable reduction of the spin polarization in the Cr atoms near the Fe-Cr frustrated bonds. In most cases, this reduction is extended up to the third to fifth Cr layer below the surface [see solutions (a), (c), (d), (e), (f), (g), (h), (j), (k) and (l) of Fe/Cr(1,0,7) in Fig. 5]. Moreover, in most of the solutions, the layered antiferromagnetic order characteristic of Cr in the ideal Fe/Cr(001) system is only recovered after the second Cr layer below the surface. This is due to spin-flip transitions that occur in Cr atoms close to the stepped interface. Experimental evidence of spin-flip transitions in Cr has been recently obtained through the magneto-optical Kerr effect by Berger and Hopster.¹⁷ The possible existence of steps at the interface was suggested as a possible explanation. The large number of solutions found for Fe/Cr(1,0,2n-1) in contrast to Cr/Fe(1,0,2n-1) and the strong propagation of the magnetic defect into the Cr substrate give clear indication that the magnetism induced by Fe is stronger than the one induced by Cr. In fact, the Cr is "accommodated" during the self-consistent procedure to the ordering imposed as a starting point for the Fe overlayer. Furthermore, those configurations which lead to antiferromagnetic order between the nearest neighbors of Fe are not possible. A spin flip occurs in those cases during the self-consistency and one of the solutions of Fig. 5 is finally recovered.

In Table II the results are reported for the average magnetizations and for the differences in total energy of the solutions shown in Fig. 5. These quantities are calculated in the same way as in the previous section. In the most stable magnetic arrangements [(a) and (b)], the average magnetization results in zero. This trend is in qualitative agreement with the absence of magnetization observed by different experimental groups in the first Fe monolayers grown on Cr(001).^{18,19} The same behavior characterizes the metastable solutions (i) and (j). In these four solutions the sign of the magnetization changes from step to step. However, it is important to note that only in the most stable configuration (b), as well as in (i), do all the Fe atoms within each step [except those at the edge in solution (a) or at the kink in (i)] display the same sign of the magnetization. As a consequence, the surface of each step constitutes a domain where the local magnetic moment points in the same direction for most of the Fe atoms. This is more evident for larger step lengths [in Fig. 6 these domains are shown for Fe/Cr(1,0,11)]. This "topological antiferromagnetism"³⁶ is in qualitative agreement with the experimental observations of Unguris *et al.*⁹ and Purcell *et al.*¹⁰ i.e., the polarization of the Fe overlayer changes from step to step (with the small period of two Cr monolayers).

In all the solutions, a reduction of the average magnetization is obtained when we consider the subsurface Cr layers in the average. This is due to the tendency of Cr to recover the antiferromagnetic order. A large variety of magnetic behaviors is obtained within the dif-

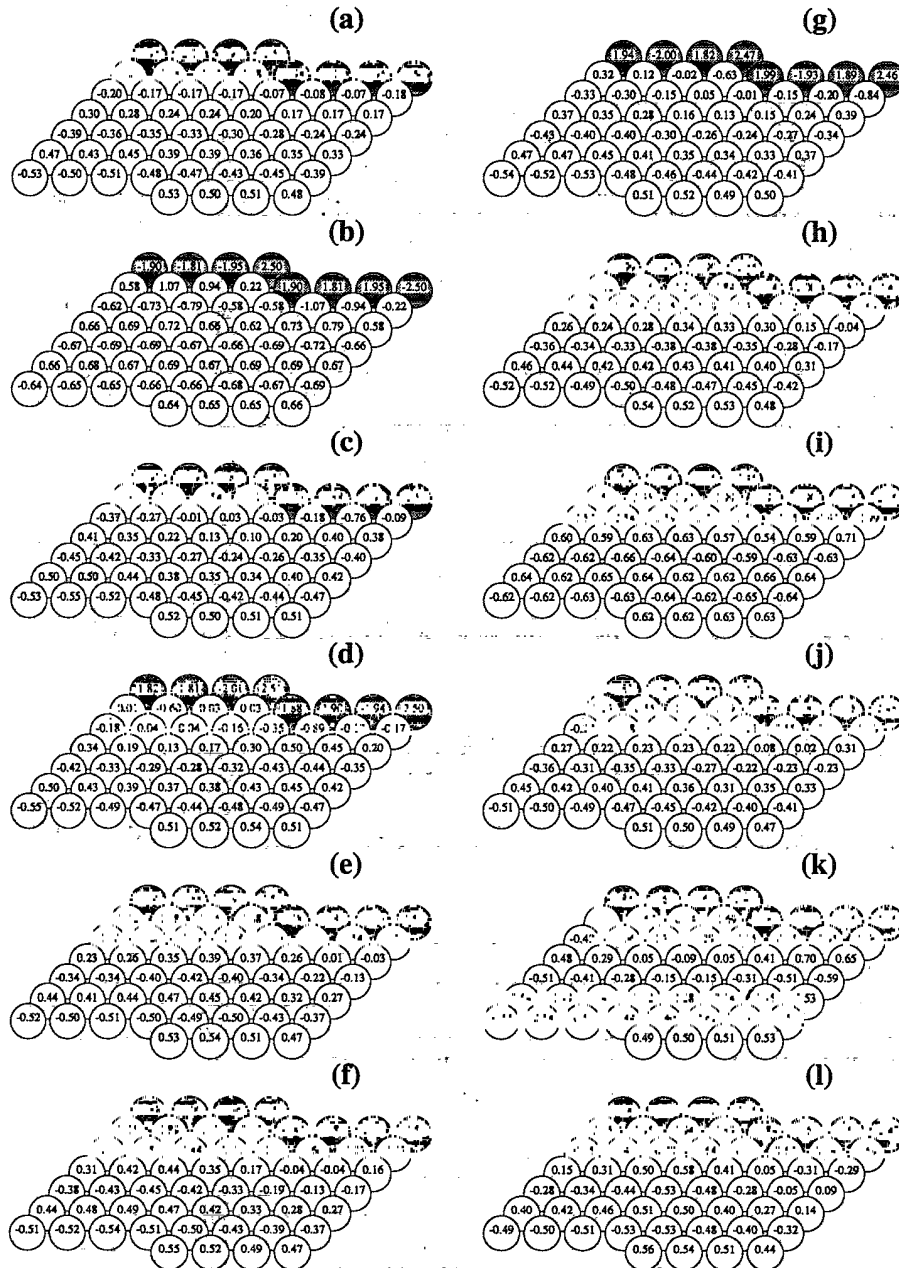


FIG. 5. Various magnetic arrangements found for Fe/Cr(1,0,7). Notice that solution (b) corresponds to that shown in Fig. 4.

TABLE II. Average magnetization per atom in the 12 solutions found for Fe/Cr(1,0,7) and shown in Fig. 5. $\bar{\mu}_i$ is the magnetization per atom when $(i - 1)$ Fe layers are averaged with the Cr overlayer. Difference in total energy (ΔE) between the metastable solutions and the stable configuration (a) taken as a reference. The difference in energy is calculated per step.

Configuration	(a)	(b)	(c)	(d)	(e)	(f)	(g)	(h)	(i)	(j)	(k)	(l)
$\bar{\mu}_1$ (μ_B)	0.00	0.00	-0.19	1.06	0.19	-1.06	1.08	-1.08	0.00	0.00	1.94	-1.94
$\bar{\mu}_2$ (μ_B)	0.00	0.00	-0.16	0.40	0.16	-0.40	0.45	-0.45	0.00	0.00	0.68	-0.68
$\bar{\mu}_3$ (μ_B)	0.00	0.00	-0.09	0.31	0.09	-0.31	0.31	-0.31	0.00	0.00	0.53	-0.53
ΔE (eV)	0.00	0.00	0.04	0.04	0.04	0.04	0.04	0.04	0.05	0.10	0.13	0.13

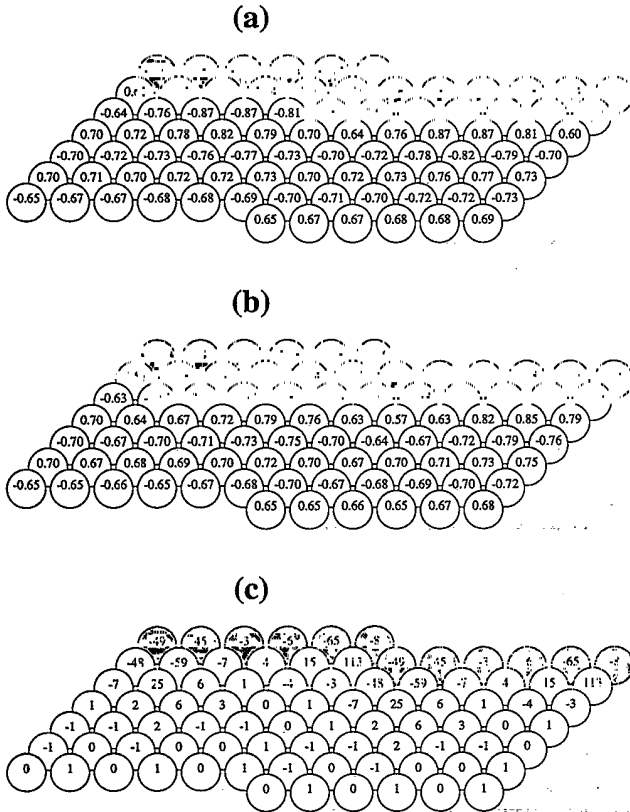


FIG. 6. The contribution of each atom to the difference in energy between the "domain arrangements," (a) and (b) for Fe/Cr(1,0,11) is illustrated in (c). Notice that the main contribution is very localized in the surrounding of the defect.

ferent solutions, i.e., positive or negative average spin polarizations, large or small average magnetizations. With respect to the relative stability, as it was the case for Cr/Fe(1,0,2n - 1), the energy necessary to change to one of the metastable configurations is very small, and some of them are degenerated (within the accuracy of the model). The difference in energy between two magnetic configurations is very localized in the atoms close to the defect. This is illustrated in Fig. 6, where we show the contribution of each atom to the difference in energy between the configurations (b) and (i) of Fe/Cr(1,0,11). The important contribution comes from the region close to the kink of the step due to the fact that the main difference between the two configurations is a spin flip in the Fe atoms at the kink and at the edge.

V. SUMMARY AND OUTLOOK

We have calculated the magnetic moments distribution for an Fe (Cr) monolayer adsorbed on different Cr (Fe) vicinal (1,0,2n - 1) substrates. The macroscopic magnitudes such as the average magnetization are traced back to the particular local magnetic moments and magnetic order within the systems. The main conclusions of this study are summarized below.

(i) In the presence of the structural defects analyzed, multiple magnetic arrangements are found, in contrast to

the case of ideal (perfectly flat) interface. The solutions differ in the different degree of frustration and in the position of the corresponding magnetic defects. In all cases, the magnetic coupling between the atoms at the edge and at the kink of the steps is the same as the coupling between the first neighbors in the corresponding bulk structures, i.e., ferromagnetic in the Fe/Cr(1,0,2n - 1) systems and antiferromagnetic in Cr/Fe(1,0,2n - 1). The number of possible magnetic configurations is larger for Fe/Cr(1,0,2n - 1) than for Cr/Fe(1,0,2n - 1) and the Cr substrate is found to be very sensitive to the magnetic defect in contrast to Fe. The difference in energy between the various solutions is small and some of them are degenerated within the accuracy of the model.

(ii) In Cr/Fe(1,0,2n - 1), a magnetic configuration with the periodicity of one step is obtained as a consequence of the strong ferromagnetism of the Fe substrate. In the most stable configuration of Cr/Fe(1,0,3), the average magnetization at the surface has the same sign as for the Fe substrate, but a transition to an antiparallel average spin polarization is obtained for Cr/Fe(1,0,5), i.e., n = 3. The presence of this type of structural defect leads to a reduction of the spin polarization of the system as compared with the ideal Cr/Fe(001). This reduction is particularly important in some metastable configurations.

(iii) In Fe/Cr(1,0,2n - 1), a magnetic configuration with the periodicity of two steps is obtained. In the two most stable magnetic arrangements, the average magnetization is zero, in qualitative agreement with the absence of magnetization observed by different experimental groups at the first Fe monolayers grown on Cr(001).^{18,19} In one of the most stable solutions, all the Fe atoms within each step (except those at the edge) display the same sign of the magnetization which oscillates from step to step. This topological antiferromagnetism is in qualitative agreement with the experimental observations of Unguris *et al.*⁹ and Purcell *et al.*¹⁰ The present result gives support to the fact that the short oscillatory period of the spin polarization of the Fe overlayer experimentally observed^{9,10} is favored by the antiferromagnetic order of the Cr substrate.

The results presented here give compelling evidence that the presence of terraces at the surface of the substrates is at the origin of some of the curious magnetic behaviors experimentally observed. However, this study constitutes only a first step. Due to the strong environmental dependence of the magnetic properties of these materials, one expects other phenomena like interdiffusion or surface reconstruction to have also an important influence in the magnetic behavior. Therefore, for a full understanding of the experiments, the geometrical structure has to be treated in the same level as the electronic structure in the calculations.

ACKNOWLEDGMENTS

A. V. would like to acknowledge the *Ministerio de Educación y Ciencia* (Spain) for financial support and the IPCMS-GEMME group for their kind hospitality. The *Institut de Physique et Chimie des Matériaux de Stras-*

bourg (IPCMS-GEMME) is "Unité Associée au Centre National de la Recherche Scientifique No. 46." The authors would like to express their gratitude to all those who have helped us to clarify our understanding of var-

ious experimental and theoretical aspects of the Fe/Cr interfaces: D. Stoeffler, J. Khalifeh, L.C. Balbás, S. Miethaner, G. Bayreuther, M. Landolt, P. Fuchs, H. Hopster, and Y. Idzerda.

*On leave from Departamento de Física Teórica, Facultad de Ciencias, Universidad de Valladolid, 47011 Valladolid, Spain.

- ¹G. Allan, *Phys. Rev. B* **19**, 4774 (1979).
- ²L. E. Klebanoff, S. W. Robey, G. Liu, and D. A. Shirley, *Phys. Rev. B* **30**, 1048 (1984); L. E. Klebanoff, R. H. Victora, L. M. Falicov, and D. A. Shirley, *ibid.* **32**, 1997 (1985).
- ³R. H. Victora and L. M. Falicov, *Phys. Rev. B* **31**, 7335 (1985).
- ⁴C. L. Fu and A. J. Freeman, *Phys. Rev. B* **33**, 1755 (1986); C. L. Fu, A. J. Freeman, and T. Oguchi, *Phys. Rev. Lett.* **54**, 2700 (1985).
- ⁵S. Ohnishi, A. J. Freeman, and M. Weinert, *Phys. Rev. B* **28**, 6741 (1983).
- ⁶A. J. Freeman and C. L. Fu, *J. Appl. Phys.* **61**, 3356 (1987).
- ⁷P. Grünberg, R. Schreiber, P. Yang, M. B. Brodsky, and H. Sowers, *Phys. Rev. Lett.* **57**, 2442 (1986).
- ⁸M. N. Baibich, J. M. Broto, A. Fert, F. Nguyen van Dau, F. Petroff, P. Etienne, G. Creuzet, A. Friedrich, and J. Chazelas, *Phys. Rev. Lett.* **61**, 2472 (1988).
- ⁹J. Unguris, R. J. Celotta, and D. T. Pierce, *Phys. Rev. Lett.* **67**, 140 (1991).
- ¹⁰S. T. Purcell, W. Folkerts, M. T. Johnson, N. W. E. McGee, K. Jager, J. van de Stegge, W. B. Zeper, and W. Honig, *Phys. Rev. Lett.* **67**, 903 (1991).
- ¹¹C. Turtur and G. Bayreuther, *Phys. Rev. Lett.* **72**, 1557 (1994), and references therein.
- ¹²F. U. Hillebrecht, Ch. Roth, R. Jungblut, E. Kisker, and A. Bringer, *Europhys. Lett.* **19**, 711 (1992).
- ¹³Y. U. Idzerda, L. H. Tjeng, H. J. Lin, C. J. Gutierrez, G. Meigs, and C. T. Chen, *Phys. Rev. B* **48**, 4144 (1993).
- ¹⁴M. Donath, D. Scholl, D. Mauri, and E. Kay, *Phys. Rev. B* **43**, 13164 (1991).
- ¹⁵D. T. Pierce, R. J. Celotta, and J. Unguris, *J. Appl. Phys.* **73**, 6201 (1993).
- ¹⁶T. G. Walker, A. W. Pang, H. Hopster, and S. F. Alvarado, *Phys. Rev. Lett.* **69**, 1121 (1992).
- ¹⁷A. Berger and H. Hopster, *Phys. Rev. Lett.* **73**, 193 (1994).
- ¹⁸C. Carbone and S. F. Alvarado, *Phys. Rev. B* **36**, 2433 (1987).
- ¹⁹G. Bayreuther (unpublished); S. Miethaner and G. Bayreuther, in Proceedings of the 14th International Colloquium on Magnetic Films and Surfaces and E-MRS Symposium on Magnetic Ultrathin Films, Multilayers and Surfaces, Düsseldorf, Germany, 1994 [J. Magn. Magn. Mater. (to be published)].
- ²⁰R. Wiesendanger, H. J. Güntherodt, G. Güntherodt, R. J. Gambino, and R. Ruf, *Phys. Rev. Lett.* **65**, 247 (1990).
- ²¹R. Haydock, in *Solid State Physics*, edited by H. Ehrenreich, F. Seitz, and D. Turnbull (Academic, New York, 1980), Vol. 35, p. 215.
- ²²D. Stoeffler and F. Gautier, *Prog. Theor. Phys. Suppl.* **101**, 139 (1990).
- ²³A. Vega, A. Rubio, L. C. Balbás, J. Dorantes-Dávila, S. Bouarab, C. Demangeat, A. Mokrani, and H. Dreyssé, *J. Appl. Phys.* **69**, 4544 (1991).
- ²⁴F. Herman, J. Sticht, and M. Van Schilfgaarde, *J. Appl. Phys.* **69**, 4783 (1991).
- ²⁵K. Hampel, D. D. Vvedensky, and S. Crampin, *Phys. Rev. B* **47**, 4810 (1993).
- ²⁶K. Lee and J. Callaway, *Phys. Rev. B* **49**, 13906 (1994).
- ²⁷C. M. Varma and A. J. Wilson, *Phys. Rev. B* **22**, 3795 (1980).
- ²⁸A. Vega, J. Dorantes-Dávila, L. C. Balbás, and G. M. Pastor, *Phys. Rev. B* **47**, 4742 (1993).
- ²⁹A. Vega, L. C. Balbás, H. Nait-Laziz, C. Demangeat, and H. Dreyssé, *Phys. Rev. B* **48**, 985 (1993).
- ³⁰L. M. Falicov, in *Magnetic Surfaces, Thin Films, and Multilayers*, edited by S. S. P. Parkin, H. Hopster, J. P. Renard, T. Shinjo, and W. Zinn, MRS Symposia Proceedings No. 231 (Materials Research Society, Pittsburgh, 1992), p. 3.
- ³¹A. Vega, L. C. Balbás, J. Dorantes-Dávila, and G. M. Pastor, *Phys. Rev. B* **50**, 3899 (1994).
- ³²A. Vega, L. C. Balbás, H. Dreyssé, and C. Demangeat, *Czech. J. Phys.* **43**, 1045 (1993).
- ³³H. Dreyssé, A. Vega, C. Demangeat, and L. C. Balbás, *Europhys. Lett.* **27**, 165 (1994).
- ³⁴A. Vega, L. C. Balbás, A. Chouairi, H. Dreyssé, and C. Demangeat, *Phys. Rev. B* **49**, 12797 (1994).
- ³⁵P. Fuchs, K. Totland, and M. Landolt, in Proceedings of the 14th International Colloquium on Magnetic Films and Surfaces and E-MRS Symposium on Magnetic Ultrathin Films, Multilayers and Surfaces, Düsseldorf, Germany, 1994 [J. Magn. Magn. Mater. (to be published)].
- ³⁶S. Blügel, D. Pescia, and P. H. Dederichs, *Phys. Rev. B* **39**, 1392 (1989).